Cardiovascular Pathology 72 (2024) 107669

Contents lists available at ScienceDirect

Cardiovascular Pathology

journal homepage: www.elsevier.com/locate/carpath

A pathological study on the efficacy of Syk inhibitors in a *Candida albicans*-induced aortic root vasculitis murine model

Nanae Asakawa[1,*], Toshiaki Oharaseki[1], Yuki Yokouchi[1], Noriko Miura[2], Naohito Ohno[3], Kei Takahashi[1]

[1] Department of Surgical Pathology (Ohashi), Toho University Graduate School of Medicine, 2-22-36, Ohashi, Meguro, Tokyo 153-8515, Japan
[2] Center for the Advance of Pharmaceutical Education, School of Pharmacy, Tokyo University of Pharmacy and Life Sciences, 1432-1 Horinouchi, Hachioji, Tokyo 192-0392 Japan
[3] School of Pharmacy, Tokyo University of Pharmacy and Life Sciences, 1432-1 Horinouchi, Hachioji, Tokyo 192-0392 Japan

ARTICLE INFO

Article history:
Received 16 January 2024
Revised 14 May 2024
Accepted 5 June 2024

Keywords:
Kawasaki disease
Vasculitis
Candida albicans
Murine model
Syk

ABSTRACT

Background: The activation of innate immunity may be involved in the development of *Candida albicans*-induced murine vasculitis, which resembles Kawasaki disease (KD) vasculitis. This study aimed to histologically clarify the time course of the development of vasculitis in this model in detail and to estimate the potential role of spleen tyrosine kinase (Syk) inhibitors in KD vasculitis.

Methods and Results: DBA/2 male mice were intraperitoneally injected with a vasculitis-inducing substance and treated with a Syk inhibitor (R788 or GS-9973). Systemic vasculitis, especially in the aortic annulus area, was histologically evaluated. Regarding lesions in the aortic annulus area, some mice in the untreated control group already showed initiation of vasculitis 1 day after the final injection of a vasculitis-inducing substance. The vasculitis expanded over time. Inflammation occurred more frequently at the aortic root than at the coronary artery. The distribution of inflammatory cells was limited to the intima, intima plus adventitia, or all layers. In the Syk inhibitor-treated groups, only one mouse had vasculitis at all observation periods. The severity and area of the vasculitis were reduced by both Syk inhibitors.

Conclusion: *Candida albicans*-induced murine vasculitis may occur within 1 day after the injection of a vasculitis-inducing substance. Additionally, Syk inhibitors suppress murine vasculitis.

1. Introduction

Kawasaki disease (KD) was first reported by Dr. Tomisaku Kawasaki in 1967 [1]. In this type of vasculitis in children, the coronary arteries are frequently affected. When a coronary aneurysm develops, thrombotic occlusion within the aneurysm can cause ischemic heart disease, which greatly affects the prognosis [1]. Histological examinations of KD autopsy cases have shown that, in coronary artery lesions, inflammatory cells infiltrate from the intimal and adventitial sides [2–4]. Additionally, on approximately the 10th day after onset of KD, vasculitis leads to tearing of the internal and external elastic lamina. When the inflammation is severe, an aneurysm is completely formed by approximately day 12 [2-4]. These findings indicate that appropriate treatment should be started by the 10th day after onset to suppress the development of cardiovascular complications such as coronary aneurysms [5]. Intravenous immunoglobulin (IVIG) therapy combined with aspirin, which is the current standard treatment for acute KD, is generally highly effective. However, 10%–20% of these patients do not respond sufficiently to IVIG and develop coronary artery complications at a high frequency [6]. Therefore, various alternative and adjunct therapies have been proposed [5]. However, at present, there is no standard second-line treatment for IVIG-resistant patients.

Although the cause of KD remains unclear, the innate immune system appears to be involved in the pathogenesis of KD. To date, three murine vasculitis models that immunohistopathologically mimic human KD vasculitis have been developed [7–11]. All of these models use pathogen-associated molecular patterns to induce vasculitis. In one of these models, a *Candida albicans* water-soluble fraction (CAWS) is used [7–9]. Studies of the CAWS model show similarity in the histology and distribution of the induced vasculitis to human KD vasculitis, as well as to the responses to IVIG and anti-tumor necrosis factor-α monoclonal antibody

* Corresponding author: Nanae Asakawa Department of Surgical Pathology (Ohashi), Toho University Graduate School of Medicine, 2-22-36, Ohashi, Meguro, Tokyo, 153-8515, Japan.
E-mail address: nanae.asakawa@med.toho-u.ac.jp (N. Asakawa).

https://doi.org/10.1016/j.carpath.2024.107669

[8,12,13]. The main constituents of CAWS are mannan, β-glucan, polysaccharides, and proteins, which are contained in the *Candida* cell wall. The administration of CAWS results in systemic vasculitis, including in the coronary arteries, in dectin-1 (β-glucan receptor)-knockout mice but not in dectin-2 (α-mannan receptor)-knockout mice [14]. Furthermore, vasculitis was not induced in mice with knockout or conditional-knockout of various molecules involved in the dectin-2-spleen tyrosine kinase (Syk)-caspase-recruitment domain 9 (CARD9) pathway [15]. These findings suggest that activation of the dectin-2-Syk-CARD9 pathway plays an important role in the onset of CAWS-induced vasculitis. However, no histological studies have reported on this murine vasculitis in the early stages of this disease.

Syk is a non-receptor tyrosine kinase that was isolated from the porcine spleen in Japan in 1991 [16]. *In vivo*, Syk is expressed mainly in hematopoietic cells and has a wide variety of roles, such as in mast cell activation and phagocytosis by macrophages [17]. In animal studies, Syk inhibitors have shown efficacy against autoimmune diseases and hematological malignancies [18,19]. In addition, multiple clinical trials of Syk inhibitors are currently being performed to treat patients with rheumatoid arteritis, IgA nephropathy, and autoimmune hemolytic anemia [20,21]. R788 is currently the only Syk inhibitor that has been clinically approved for treatment of chronic idiopathic thrombocytopenic purpura in the United States, Canada, Europe, and Japan [22]. On the other hand, there is increasing interest in GS-9973, which showed higher Syk specificity than R788 in *in vitro* experiments [23].

This histological study aimed to develop CAWS-induced vasculitis in mice, especially focusing on its early stage, and to determine the effects of two Syk inhibitors on vasculitis. Our findings will hopefully help determine the potential of Syk inhibitors in the treatment of vasculitis in patients with KD.

2. Materials and methods

2.1. Animals

Four-week-old male DBA/2 mice were purchased from Sankyo Labo Service Corporation Inc. (Edogawa, Tokyo, Japan) and used in experiments after 1 week of acclimatization. The animal room was maintained at 23°C±2°C and 60%–70% relative humidity. The mice were fed a commercial diet (CLEA Rodent Diet CE-2; CLEA Japan Inc. [Meguro, Tokyo, Japan]) and had free access to tap water. All procedures were performed in compliance with the relevant laws and institutional guidelines. The study design was approved by Toho University's Animal Ethics (Approval No. 19-51-425).

2.2. Vasculitis-inducing substances

As reported previously [8], *C. albicans* (NBRC1385) was cultured in a complete synthetic medium, and CAWS was derived from the culture supernatant. CAWS 200 μg was dissolved in 0.2 mL of phosphate-buffered saline (PBS) and injected into the peritoneal cavity of mice for 5 consecutive days.

2.3. Syk inhibitors

Two Syk inhibitors were used, namely R788 (#A144826; Ambeed, Inc. [Arlington Heights, IL, USA]) and GS-9973 (#181632; Ambeed, Inc.).

2.4. Experimental schedule

In the R788 group (R group), 0.8 mg of R788 was suspended in 0.1 ml of solvent and administered intraperitoneally to mice twice daily starting from the day after the final CAWS injection. The following two R subgroups had different R788 administration periods. In the R-1w subgroup (n=10), R788 was administered for 1 week, and in the R-3w subgroup (n=10), R788 was administered for 3 weeks.

In the GS-9973 group (G group), 1 mg of GS-9973 was suspended in 0.1 ml of solvent and administered intraperitoneally to mice once daily starting from the day after the final CAWS injection. The following two G subgroups had different GS-9973 administration periods. In the G-1w subgroup (n=10), GS-9973 was administered for 1 week, and in the G-3w subgroup (n=10), GS-9973 was administered for 3 weeks. In the control group (C group), each subgroup (n=10) for comparison with the R and G subgroups only received solvent after the CAWS injection.

In the control C-1w and C-3w subgroups, administration of solvent was performed once or twice daily to match administration in the corresponding Syk inhibitor treatment groups. So, C-1w (n=10) and C-3w (n=10) subgroups that matched R group received solvent twice daily, and C-1w (n=10) and C-3w (n=10) subgroups that matched G group received solvent once daily. To examine the initiation of CAWS-induced vasculitis, the C-1d subgroup (n=11), which was administered neither Syk inhibitor nor solvent, was used. Mice in this subgroup were euthanized 1 day after the final CAWS administration for later histological analysis.

The solvent was a mixture of 0.5% carboxymethyl cellulose + 0.25% polysorbate 80. The doses of R788 and GS-9973 used in this experiment correspond to the maximum doses previously administered to mice [24,25].

All mice were euthanized with carbon dioxide after the final administration of the solvent or Syk inhibitor. The mice were then necropsied, and their hearts, lungs, liver, pancreas, spleen, kidneys, abdominal aorta to common iliac artery, and testes were harvested and fixed in neutral buffered formalin for histological examination.

2.5. Histological analysis of vasculitis

2.5.1. Histological and immunohistochemical analysis

Formalin-fixed organs were embedded in paraffin. For hearts, serial sections of the aortic annulus area were prepared, including the origins of the left and right coronary arteries. Hematoxylin and eosin (HE) staining and elastica van Gieson staining were performed. The aortic annulus area was divided into five segments of the left coronary artery, left coronary sinus, non-coronary sinus, right coronary sinus, and right coronary artery. The degree of inflammation in each segment was classified into four grades as follows: Grade 0, no inflammation; Grade 1, inflammatory cell infiltration limited to one layer (i.e., the intima, media, or adventitia); Grade 2, inflammatory cell infiltration limited to two layers among the intima, media, and adventitia; and Grade 3, inflammatory cell infiltration involving all three layers (vasculitis). The degree of inflammation was assessed by two observers independently. If the two observers could not reach a consensus, a third person provided an opinion.

Immunohistochemical staining was also performed to identify macrophages using anti-F4/80 antibody (clone D2S9R; Cell Signaling technology [Danvers, MA, USA]). The sections were visualized with the high polymer method (Histofine Simple Stain Mouse, Rabbit MAX-PO; Nichirei Bioscience [Chuo, Tokyo, Japan]) and colorized with diaminobenzidine chromogen.

Tissue sections of organs, except for the hearts were stained with hematoxylin and eosin. The presence or absence of vasculitis was examined.

2.5.2. Semi-quantitative and quantitative histological measurements

The following items were compared between the experimental groups. (1) The incidence of vasculitis was determined by

the percentage of mice with vasculitis (Grade 3) in each group. (2) The severity of vasculitis was determined by the sum of the inflammation Grades in each of the five segments for each mouse. (3) To determine the area of vasculitis for each mouse, the specimen containing the lesion area with the greatest two-dimensional extent of inflammation was chosen. The area of the lesion observed in each selected specimen was treated as "the area of vasculitis." The area of vasculitis may have extended over two or more segments. The area of vasculitis was measured using the image analysis/measurement software WinRoof 2018, version 4.25.10 (Mitani Co. [Kanazawa, Ishikawa, Japan]).

2.6. Statistical analysis

A non-parametric method was used for the analysis. The Fisher's exact test was used to compare the incidence of vasculitis between the mouse groups. The Kruskal–Wallis test was used to compare the severity and area of vasculitis. When a significant between-group variation was observed in the Kruskal–Wallis test, a post-hoc test was performed using Dunn's multiple comparison test. All test results were considered significant at $P<.05$.

3. Results

3.1. Histological and immunohistochemical analysis of vasculitis

All mice used in the experiment survived. In each segment, we first observed the aortic annulus area histologically and then classified the degree of inflammation into the four grades described above (Fig. 1). Generally, although right coronary sinus, non-coronary sinus, and left coronary sinus lesions tended to occur at the base of the aortic valve or coronary artery origin, few mice had inflammation in the aortic root, which had no connection to the aortic valve or in the coronary artery removed from the ostium. All Grade 1 lesions consisted of inflammation limited to the intima (Fig. 2A), while all Grade 2 lesions consisted of inflammation limited to the intima and adventitia (Fig. 2B). Grade 3 lesions consisted of inflammation invading all layers, but the density of inflammatory cells and destruction of vascular wall structure showed different degrees (Figs. 2C and D). Regardless of the grades, the inflammatory cells observed in the vascular lesions were mainly large mononuclear cells, which were immunohistochemically shown as F4/80-positive macrophages (Figs. 2A–D).

C-1d

#	LCA	LCS	NCS	RCS	RCA
1	0	2	2	1	0
2	1	1	2	2	0
3	0	3	3	2	0
4	2	1	2	2	0
5	0	1	1	1	0
6	0	0	1	1	0
7	0	1	2	3	0
8	0	1	1	1	0
9	1	2	1	1	0
10	0	1	2	2	0
11	1	2	1	2	0

Grade 0
Grade 1
Grade 2
Grade 3

C-1w

#	LCA	LCS	NCS	RCS	RCA
1	3	0	0	2	3
2	0	0	1	0	1
3	0	1	1	1	0
4	3	3	3	0	0
5	0	1	2	2	0
6	0	3	3	2	0
7	0	1	0	0	0
8	0	1	0	0	0
9	0	3	3	0	0
10	0	1	1	0	0

C-1w

#	LCA	LCS	NCS	RCS	RCA
1	0	0	3	3	0
2	0	1	0	0	0
3	2	1	1	3	0
4	0	1	3	3	0
5	0	0	3	3	0
6	0	1	1	3	3
7	0	1	2	0	0
8	0	1	3	3	0
9	0	0	0	0	0
10	3	2	3	3	0

R-1w

#	LCA	LCS	NCS	RCS	RCA
1	0	0	0	0	0
2	0	0	0	0	0
3	0	0	1	1	1
4	0	0	0	1	0
5	0	1	1	1	0
6	0	1	1	0	0
7	0	0	3	1	0
8	0	0	0	0	0
9	0	1	1	0	0
10	1	1	1	0	0

G-1w

#	LCA	LCS	NCS	RCS	RCA
1	0	1	1	0	0
2	0	1	0	0	0
3	0	0	0	0	0
4	0	0	0	0	0
5	0	1	1	1	0
6	0	0	0	0	0
7	0	0	0	1	0
8	0	0	0	0	0
9	0	0	0	0	0
10	0	0	1	0	0

C-3w

#	LCA	LCS	NCS	RCS	RCA
1	0	1	1	1	0
2	3	3	3	3	3
3	1	1	3	1	0
4	3	3	1	1	0
5	0	1	1	0	0
6	0	1	2	2	0
7	0	3	3	0	0
8	0	0	3	3	0
9	0	3	3	3	0
10	0	1	1	1	0

C-3w

#	LCA	LCS	NCS	RCS	RCA
1	0	3	3	0	0
2	0	0	0	1	0
3	0	1	0	2	3
4	0	0	3	3	0
5	3	3	1	0	0
6	0	0	3	3	3
7	0	0	0	3	3
8	0	0	0	1	0
9	0	0	0	0	1
10	0	1	1	0	0

R-3w

#	LCA	LCS	NCS	RCS	RCA
1	0	0	0	0	0
2	0	0	0	1	0
3	0	1	0	0	0
4	0	1	1	0	0
5	0	0	2	0	0
6	0	1	2	1	0
7	0	2	0	1	0
8	0	1	1	0	0
9	0	1	1	1	0
10	0	1	1	1	0

G-3w

#	LCA	LCS	NCS	RCS	RCA
1	0	1	0	0	0
2	0	0	0	0	0
3	0	0	0	0	0
4	0	0	0	0	0
5	0	0	1	0	0
6	0	0	1	0	0
7	0	1	0	0	0
8	0	0	0	1	0
9	0	0	0	0	0
10	0	0	0	0	0

Fig. 1. Degree of inflammation in each segment of the aortic annulus area. The aortic annulus area was divided into five segments of the left coronary artery, left coronary sinus, non-coronary sinus, right coronary sinus, and right coronary artery. The inflammation Grade (0–3) is shown for each of the five segments of all mice. Data are shown for each experimental group. LCA: left coronary artery; LCS: left coronary sinus; NCS: non-coronary sinus; RCS: right coronary sinus; RCA: right coronary artery.

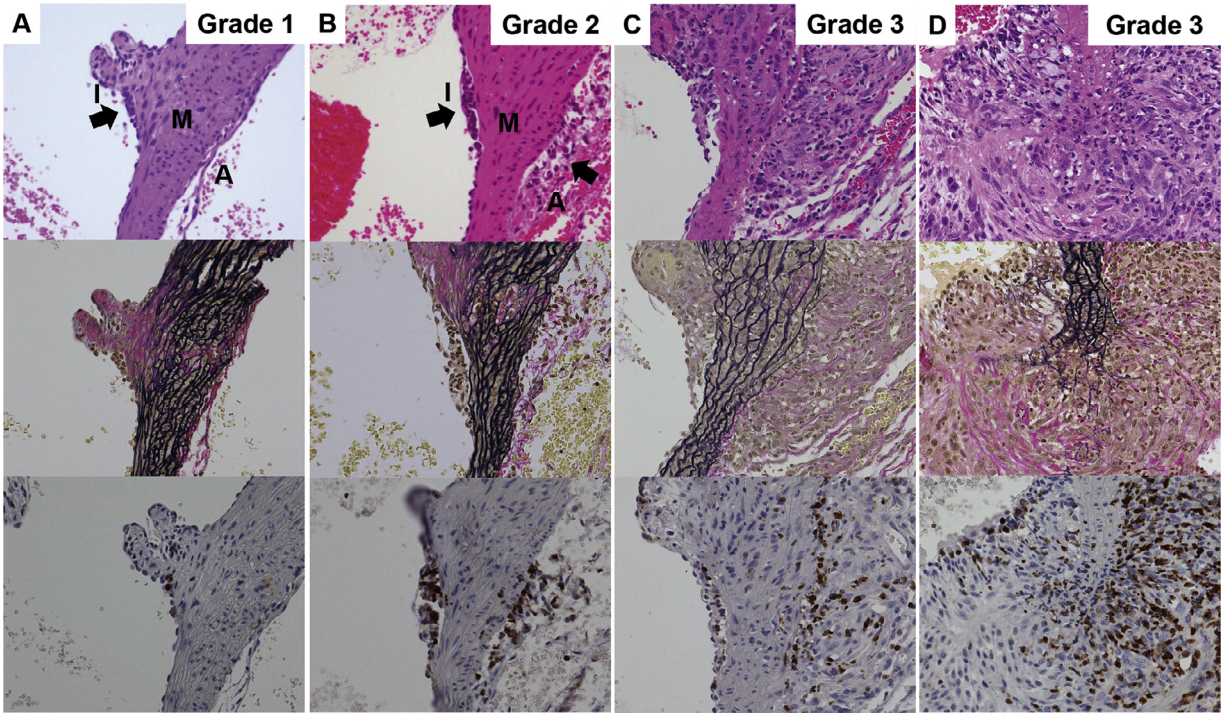

Fig. 2. Representative histology of each grade. (A, upper and middle panels) A Grade 1 lesion in the C-1d subgroup shows a few large mononuclear cells attached to endothelial cells. (B, upper and middle panels) A Grade 2 lesion in the C-1w subgroup shows localized cellular intimal thickening and mild adventitial inflammation. (C, upper and middle panels) A Grade 3 lesion in the C-1w subgroup shows marked thickening of the intima, media, and adventitia owing to moderate inflammatory cell infiltration with separation of the elastic fibers. (D, upper and middle panels) A Grade 3 lesion in the C-3w subgroup shows severe inflammation, and separation and rupture of the elastic fibers. The black arrows indicate large mononuclear cells. (A–D, lower panels) The inflammatory cells mainly expressed F4/80 from the early phase to the peak of the inflammation. I: intima, M: media, A: adventitia. Upper panels: hematoxylin and eosin stain, middle panels: elastica van Gieson stain, lower panels: F4/80 immunohistochemical stain.

Except for the aortic annulus area, vasculitis was observed only in the origin of the renal artery (Supplemental Figure 1). Vasculitis of the renal artery was observed in 10% (n=1/10) of C-1w mice and 15% (n=3/20) of C-3w mice. No mice in the R group or G group had inflammatory lesions in any organ other than the aortic annulus area.

3.1.1. C group

Each of the C groups matched with the R group and to the G group showed similar lesions. In the C groups, grade 1 lesions had a few inflammatory cells attached to endothelial cells, with mild endothelial cell swelling. No fibro-cellular intimal proliferation was observed (Fig. 2A). In Grade 2 lesions, nodular accumulation of inflammatory cells in several overlapping layers and localized thickening were observed in the intima, while mild edematous changes and infiltration of inflammatory cells were observed in the adventitia (Fig. 2B). However, Grade 3 lesions showed various types of histology depending on the time from the CAWS injection. In the C-1d subgroup, although inflammatory cell infiltration was observed in all three vascular wall layers, the degree was extremely mild and localized, and there was no rupture of elastic fibers or breakdown of the vascular wall structure (Supplemental Figure 2). In the C-1w and C-3w subgroups, marked thickening of the vascular wall due to moderate to severe inflammatory cell infiltration, with separation and rupture of the elastic fibers, was observed. (Figs. 2C and D, Supplemental Figure 3B). Regarding the mice with Grade 3 lesions, clear destruction of the vascular wall structure was observed in 0% (0/2) of C-1d mice, 55% (6/11) of G-1w mice, and 100% (12/12) of C-3w mice. No fibrinoid necrosis was observed.

3.1.2. R group

Grade 1 lesions in the R group were similar to those in the C group. In all of the Grade 2 lesions in R-3w subgroup mice (n=3), inflammatory cells that infiltrated into the intima and adventitia were less dense than those in Grade 2 lesions in the C-3w subgroup (Fig. 3B). In the R group, only one mouse in the R-1w subgroup had a Grade 3 lesion, and the density of inflammatory cells was lower and there was no vascular wall destruction compared with the C-1w subgroup (Supplemental Figure 4).

3.1.3. G group

There were no Grade 2 or Grade 3 lesions in the G-1w or G-3w subgroup. The only inflammatory lesions observed were Grade 1, which were similar to those in the C groups (Fig. 3C). There was no disruption of the vascular wall structure.

3.2. Semi-quantitative and quantitative studies of vasculitis: incidence, severity, and area of vasculitis

There was no significant difference in the incidence or severity of vasculitis between the three C subgroups (Figs. 4A and B). Comparison of the area of vasculitis between the three C subgroups showed that it was larger in the 3w subgroup than in the 1d subgroup (P=.04) (Fig. 4C).

When the C and R subgroups were compared, the incidence and severity of vasculitis in the R-3w subgroup were lower than those in the C-3w subgroup (P=.01 and P<.01, respectively) (Figs. 5A and C). The area of vasculitis was smaller in each of the R subgroups than in each of the C subgroups (R-1w subgroup: P=.03; R-3w subgroup: P<.01) (Fig. 5E).

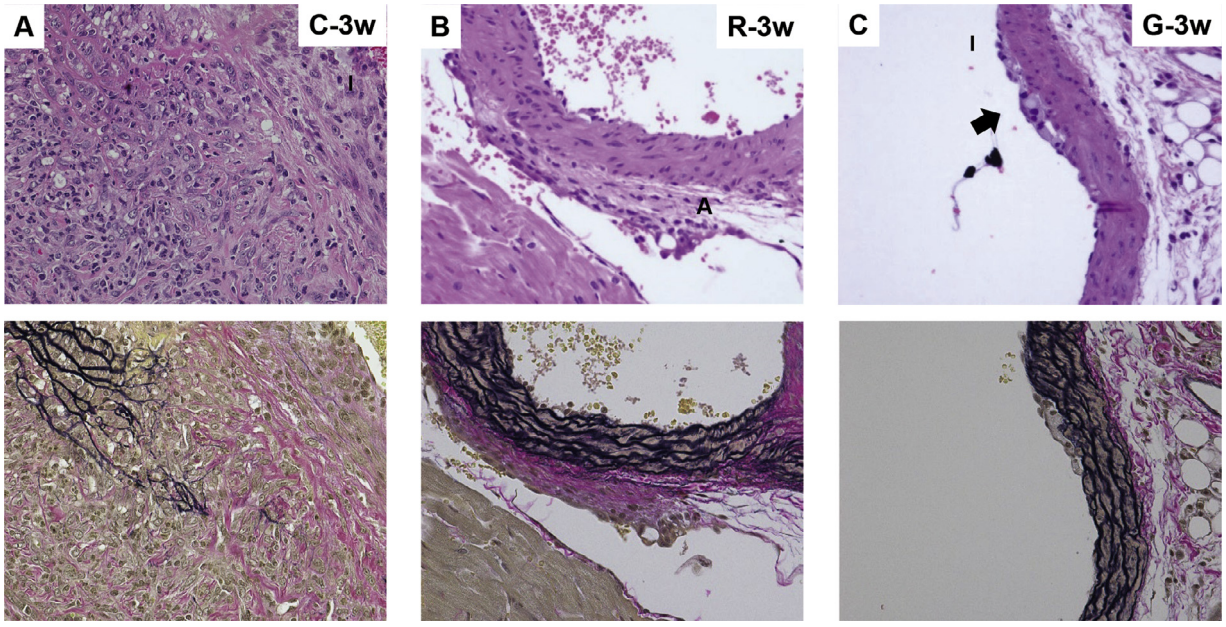

Fig. 3. Histology of inflammatory lesions in each experimental group. (A) Aortic annulus area in the C-3w subgroup. The extent of inflammation and the density of inflammatory cells tended to increase with time, and thickening and breakdown of the vascular wall structure progressed. (B) Aortic annulus area in the R-3w subgroup. At 3 weeks, some mice had developed Grade 2 lesions, but no breakdown of the vascular wall structure was observed. **(C)** Aortic annulus area in the G-3w subgroup. When inflammatory cell infiltration was observed, it involved only the intima, and there was no breakdown of the vascular wall structure. The black arrows indicate inflammation in the intima. I: intima; A: adventitia. Upper panels: hematoxylin and eosin stain, lower panels: elastica van Gieson stain.

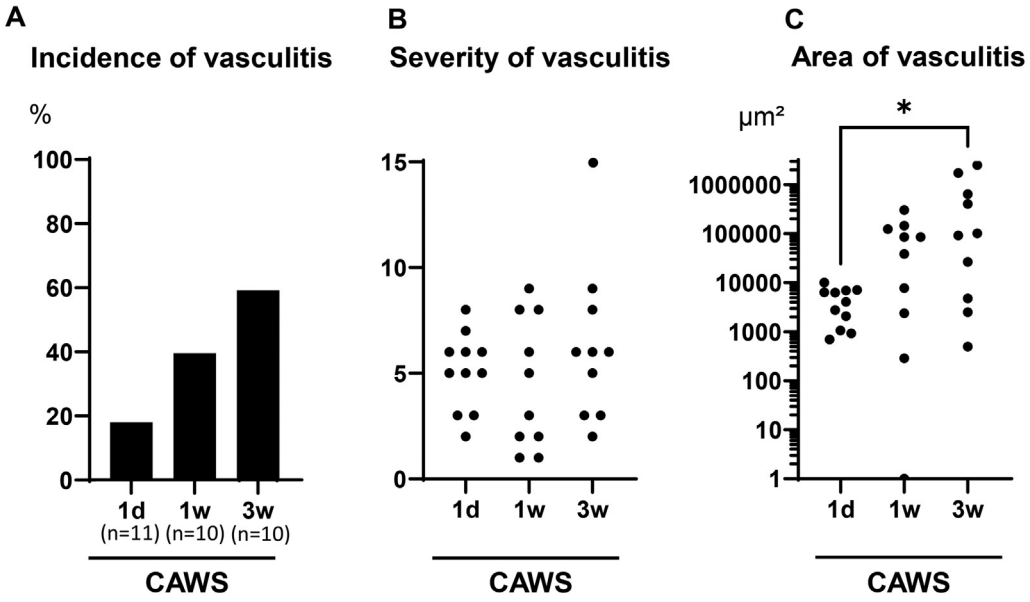

Fig. 4. Semi-quantitative and quantitative studies of vasculitis over time in the C subgroups. (A) Incidence of vasculitis. No significant difference in the incidence of vasculitis was observed between the three subgroups (n=10-11/subgroup). Data were analyzed by the Fisher's exact test. (B) Severity of vasculitis. No significant difference in the severity of vasculitis was found between the subgroups. Data were analyzed by the Kruskal–Wallis test. (C) Area of vasculitis. Data were analyzed by the Kruskal–Wallis test with Dunn's multiple comparison test. $^{*}P<.05$.

When the C and G subgroups were compared, each of the G subgroups had a lower incidence and severity of vasculitis than the C subgroups (G-1w and G-3w subgroups: all $P<.05$) (Fig. 5B and D). Additionally, the area of vasculitis was smaller in each of the G subgroups than in the C subgroups (G-1w and G-3w subgroups: both $P<.01$) (Fig. 5F).

4. Discussion

The time course of the development of CAWS vasculitis in DBA/2 mice has been previously reported. Hirata et al. administered a single dose of 1 mg or 4 mg of CAWS intraperitoneally to DBA/2 mice for 5 consecutive days [26]. They found inflammatory cell infiltration from the adventitia to the media of the aortic annulus lesion 1 week after the final CAWS injection at both doses, and observed that inflammation worsened with time. In their study, vasculitis was described as severe inflammation that involved the entire aortic annulus area. However, no studies have reported in detail on the initial lesion. Therefore, to clarify the histology of initial CAWS-induced vasculitis, we observed serial sections of the aortic annulus area that had been obtained from CAWS-treated control mice 1 day, 1 week, and 3 weeks after the

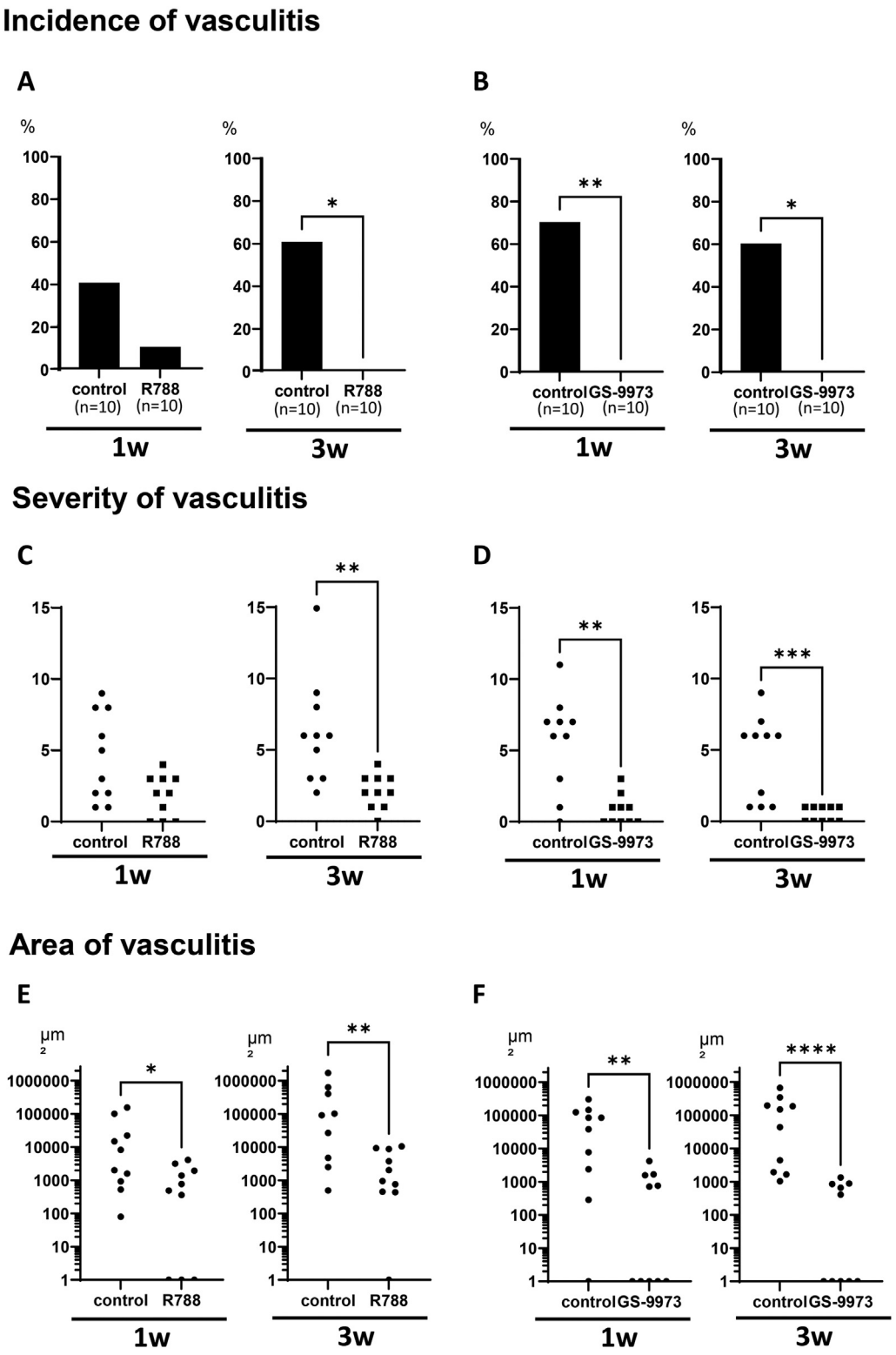

Fig. 5. Responses to each Syk inhibitor treatment. Comparison of the C, R, and G groups. Each of the 1w and 3w subgroups showed similar trends (n=10/subgroup). (A, B) Incidence of vasculitis, (C, D) severity of vasculitis, and (E, F) area of vasculitis. Data were analyzed by the Fisher's exact test (A, B) or by the Kruskal–Wallis test with Dunn's multiple comparison test (C–F). $^{*}P<.05$, $^{**}P<.01$, $^{***}P<.001$, $^{****}P<.0001$.

final CAWS injection. We found that 1 day after the final CAWS injection, all mice already showed varying degrees of inflammation, ranging from intimal inflammation to vasculitis. However, no lesions showed breakdown of the vascular wall structure at that time. After 1 day, the vasculitis became larger and the vascular wall structure was destroyed over time. Additionally, we found that the distribution of inflammatory cells induced in the vascular wall by CAWS could be classified as intima, the intima plus adventitia, and all three layers. There were no findings of inflammatory cell infiltration of only the media or only the adventitia, the

intima plus media, or the media plus adventitia. These findings indicate that, in the CAWS-induced vasculitis murine model, inflammation starts in the intima, followed by inflammatory cell infiltration of the adventitia, and then it further spreads to the media, thereby culminating in vasculitis. Intimal inflammation that was the earliest manifestation of vasculitis observed in our study was a small lesion with only a few inflammatory cells adhering to the intima. Such small lesions can be discovered only by preparing serial sections and carefully observing them, and they may have been overlooked in previous studies. We were concerned that evaluating the therapeutic effect of Syk inhibitors might be difficult if the induced inflammation was too severe. Therefore, we adjusted the dose of CAWS for more optimal evaluation of the effects of treatment. Consequently, the incidence of vasculitis in the CAWS-injected control group (C group) was limited to approximately 60% from 1 to 3 weeks after the final CAWS injection. Additionally, few mice had severe inflammation, such as that observed in previous studies [26]. Moreover, in this study, inflammation occurred more frequently at the aortic root than at the coronary artery, especially at the base of aortic valve or the coronary artery origin. Notably, this distribution is different from KD vasculitis. The cause of this difference is unclear, but CAWS vasculitis may commonly occur at the base of the aortic valve and coronary artery origin. The inflammation may then spread to the entire circumference of the aortic root, including the coronary arteries. Alternatively, this difference may have been caused by the low CAWS dose in our study. Furthermore, although vasculitis was observed at the renal artery origin, the frequency was markedly lower than that at the aortic annulus area.

In this study, administration of the two Syk inhibitors reduced vasculitis, suggesting that Syk is a potential target for treatment of vasculitis. The effects of the Syk inhibitors were evaluated based on histology of the aortic annulus area. We found that a small number of mice had residual inflammation in the aortic annulus area even after treatment with a Syk inhibitor. However, in each case, the degree of inflammatory cell infiltration was mild, and no vascular wall structure breakdown was observed. Additionally, no mice that had been treated by either Syk inhibitor had vasculitis of any organ other than the heart. A vasculitis-reducing effect of Syk inhibitors was observed at 1 week after starting treatment, suggesting that activation of Syk is involved in the early stage of development of CAWS-induced vasculitis. To suppress occurrence of complications, such as coronary aneurysms due to destruction of the vascular wall structure, completing effective administration in the early stages of inflammation is necessary. This requirement also applies to therapeutic intervention using Syk inhibitors. There is concern that long-term use of Syk inhibitors may lead to adverse events, including infections, because of the various roles of Syk in immunologically relevant pathways *in vivo* [17]. However, in the case of KD, which is an acute inflammatory disease, treatment is likely to be short term, and Syk inhibitors can potentially be useful in treating vasculitis [27].

R788 and GS-9973 suppress activity of Syk by competitively inhibiting ATP binding. However, the Syk inhibitors that have been developed to date cannot be considered to be specific for Syk. The reason for this lack of specificity is that the kinase domain of the protein kinase that includes Syk has amino acid homology. Therefore, even a kinase inhibitor that shows high specificity for Syk *in vitro* may also affect other kinases and sometimes even non-kinases *in vivo* [28]. Consequently, Syk inhibitors have the potential to exert a wide range of pharmacological effects beyond their reach. In this study, we found that inflammatory cell infiltration was limited to only the intima in the aortic annulus area in the GS-9973 group, which showed higher Syk selectivity. However, inflammation occurred not only in the intima, but also in the adventitia and media, in the R788 group. These findings support the concept that Syk plays an important role in the development of CAWS-induced vasculitis.

In summary, the initiation of CAWS-induced vasculitis in the coronary annulus area of DBA/2 mice was observed by 1 day after the final CAWS injection. Inflammatory cell infiltration spread to the intima, and then to the adventitia and media. The destruction of the vascular wall structure accompanied by rupture of elastic fibers occurred after more than 1 week after the final CAWS injection. Syk inhibitor treatment, which started from 1 day after the final CAWS injection, suppressed not only the progression of vasculitis but also destruction of the vascular wall structure, and reduced the area of inflammatory lesions. GS-9973, which has higher Syk selectivity than R788, showed a stronger vasculitis-reducing effect than R788.

Declaration of competing interest

None.

CRediT authorship contribution statement

Nanae Asakawa: Writing – review & editing, Writing – original draft, Validation, Project administration, Methodology, Investigation, Funding acquisition, Formal analysis, Data curation, Conceptualization. **Toshiaki Oharaseki:** Writing – review & editing, Methodology, Investigation. **Yuki Yokouchi:** Writing – review & editing, Methodology, Investigation. **Noriko Miura:** Writing – review & editing, Resources, Methodology. **Naohito Ohno:** Writing – review & editing, Resources, Methodology. **Kei Takahashi:** Writing – review & editing, Validation, Supervision, Project administration, Methodology, Conceptualization.

Funding

This work was supported by the Toho University School of Medicine Project Research Funds [grant numbers 19-23 and 20-05]; and a 2021 Research Grant of Japan Kawasaki Disease Research Center.

Acknowledgments

We would like to thank Yoshie Muraishi for technical assistance. We thank Ellen Knapp, PhD, from Edanz (https://jp.edanz.com/ac) for editing a draft of this manuscript.

Supplementary materials

Supplementary material associated with this article can be found, in the online version, at doi:10.1016/j.carpath.2024.107669.

References

[1] Kawasaki T, Kosaki F, Okawa S, Shigematsu I, Yanagawa H. A new infantile acute febrile mucocutaneous lymph node syndrome (MLNS) prevailing in Japan. Pediatrics 1974;54(3):271–6.
[2] Amano S, Hazama F, Kubagawa H, Tasaka K, Haebara H, Hamashima Y. General pathology of Kawasaki disease: on the morphological alterations corresponding to the clinical manifestations. Acta Pathol Jpn 1980;30:681–94.
[3] Y Yuki, Oharaseki T, Enomoto Y, Sato W, Imanaka YK, Takahashi K. Expression of tenascin C in cardiovascular lesions of Kawasaki disease. Cardiovasc Pathol 2019;38:25–30. doi:10.1016/j.carpath.2018.10.005.
[4] Sato W, Yokouchi Y, Oharaseki T, Asakawa N, Takahashi K. The pathology of Kawasaki disease aortitis: a study of 37 cases. Cardiovasc Pathol 2021;51:107303. doi:10.1016/j.carpath.2020.107303.
[5] McCrindle BW, Rowley AH, Newburger JW, Burns JC, Bolger AF, Gewitz M, et al. Diagnosis, treatment, and long-term management of Kawasaki disease: a scientific statement for health professionals from the American Heart Association. Circulation. 2017;135:e927–99. doi:10.1161/CIR.0000000000000484.
[6] Kobayashi T, Inoue Y, Takeuchi K, Okada Y, Tamura K, Tomomasa T, et al. Prediction of intravenous immunoglobulin unresponsiveness in patients with Kawasaki disease. Circulation 2006;13:2606–12. doi:10.1161/CIRCULATIONAHA.105.592865.

[7] Murata H, Naoe S. Experimental *Candida*-induced arteritis in mice– relation to arteritis in Kawasaki disease. Prog Clin Biol Res 1987;250:523.
[8] Ohno N. Murine model of Kawasaki disease induced by Mannoprotein-β-Glucan complex, CAWS, obtained from *Candida albicans*. Jpn J Infect Dis 2004;57(5):S9–10.
[9] Yoshikane Y, Koga M, Imanaka YK, Cho T, Yamamoto Y, Yoshida T, et al. JNK is critical for the development of Candida albicans-induced vascular lesions in a mouse model of Kawasaki disease. Cardiovasc Pathol 2015;24(1):33–40. doi:10.1016/j.carpath.2014.08.005.
[10] Lehman TJ, Mahnovski V. Animal models of vasculitis. Lessons we can learn to improve our understanding of Kawasaki disease. Rheum Dis Clin North Am 1988;14(2):479–87.
[11] Nishio H, Kanno S, Onoyama S, Ikeda K, Tanaka T, Kusuhara K, et al. Nod1 ligands induce site-specific vascular inflammation. Arterioscler Thromb Vasc Biol 2011;31(5):1093–9.
[12] Takahashi K, Oharaseki T, Yokouchi Y, Miura NN, Ohno N, Okawara AI, et al. Administration of human immunoglobulin suppresses development of murine systemic vasculitis induced with *Candida albicans* water-soluble fraction: an animal model of Kawasaki disease. Mod Rheumatol 2010;20(2):160–7. doi:10.1007/s10165-009-0250-5.
[13] Oharaseki T, Yokouchi Y, Yamada H, Mamada H, Muto S, Sadamoto K, et al. The role of TNF-α in a murine model of Kawasaki disease arteritis induced with a *Candida albicans* cell wall polysaccharide. Mod Rheumatol 2014;24(1):120–8. doi:10.3109/14397595.2013.854061.
[14] Oharaseki T, Yokouchi Y, Enomoto Y, Sato W, Ishibash K, Miura N, et al. Recognition of alpha-mannan by dectin 2 is essential for onset of Kawasaki disease-like murine vasculitis induced by *Candida albicans* cell-wall polysaccharide. Mod Rheumatol 2020;30(2):350–7. doi:10.1080/14397595.2019.1601852.
[15] Miyabe C, Miyabe Y, Bricio-Moreno L, Lian J, Rahimi RA, Miura NN, et al. Dectin-2–induced CCL2 production in tissueresident macrophages ignites cardiac arteritis. J Clin Invest 2019;129(9):3610–24. doi:10.1172/JCI123778.
[16] Sakai K, Nakamura S, Sada K, Kobayashi T, Uno H, Yamamura H. Characterization of partially purified cytosolic protein-tyrosine kinase from porcine spleen. Biochem Biophys Res Commun 1988;152(3):1123–30. doi:10.1016/s0006-291x(88)80401-7.
[17] Riccaboni M, Bianchi I, Petrillo P. Spleen tyrosine kinases: biology, therapeutic targets and drugs. Drug Discov Today 2010;15(13-14):517–30. doi:10.1016/j.drudis.2010.05.001.
[18] McAdoo SP, Prendecki M, Tanna A, Bhatt T, Bhangal G, McDaid J, et al. Spleen tyrosine kinase inhibition is an effective treatment for established vasculitis in a pre-clinical model. Kidney Int 2020;97(6):1196–207. doi:10.1016/j.kint.2019.12.014.
[19] Sprissler C, Belenki D, Maurer H, Aumann K, Pfeifer D, Klein C, et al. Depletion of STAT5 blocks TEL–SYK-induced APMF-type leukemia with myelofibrosis and myelodysplasia in mice. Blood Cancer J 2014;4(8):e240. doi:10.1038/bcj.2014.53.
[20] Weinblatt ME, Genovese MC, Ho M, Hollis S, Rosiak-Jedrychowicz K, Kavanaugh A, et al. Effects of fostamatinib, an oral spleen tyrosine kinase inhibitor, in rheumatoid arthritis patients with an inadequate response to methotrexate. Arthritis Rheumatol 2014;66(12):3255–64. doi:10.1002/art.38851.
[21] Markham A. Fostamatinib: first Global Approval. Drugs 2018;78(9):959–63. doi:10.1007/s40265-018-0927-1.
[22] Connell NT, Berliner N. Fostamatinib for the treatment of chronic immune thrombocytopenia. Blood 2019;133(19):2027–30. doi:10.1182/blood-2018-11-852491.
[23] Currie KS, Kropf JE, Lee T, Blomgren P, Xu J, Zhao Z, et al. Discovery of GS-9973, a selective and orally efficacious inhibitor of spleen tyrosine kinase. J Med Chem 2014;8:57(9):3856–73. doi:10.1021/jm500228a.
[24] Zhu Y, Herlaar E, Masuda ES, Burleson GR, Nelson AJ, Grossbard EB, et al. Immunotoxicity assessment for the novel Spleen tyrosine kinase inhibitor R406. Toxicol Appl Pharmacol 2007;221:268–77. doi:10.1016/j.taap.2007.03.027.
[25] Yoshimoto T, Hayashi T, Kondo T, Kittaka M, Reichenberger EJ, Ueki Y. Second-generation SYK inhibitor entospletinib ameliorates fully established inflammation and bone destruction in the Cherubism Mouse Model. J Bone and Miner Res 2018;33(8):1513–19. doi:10.1002/jbmr.3449.
[26] Hirata N, Ishibashi K, Usui T, Yoshioka J, Hata S, Adachi Y, et al. A model of left ventricular dysfunction complicated by CAWS arteritis in DBA/2 mice. Int J Vasc Med 2012;2012:570297. doi:10.1155/2012/570297.
[27] Ae R, Makino N, Kosami K, Kuwabara M, Matsubara Y, Nakamura Y. Epidemiology, treatments, and cardiac complications in patients with Kawasaki disease: the Nationwide Survey in Japan, 2017-2018. J Pediatr 2020;225:23–9. doi:10.1016/j.jpeds.2020.05.034.
[28] Karaman MW, Herrgard S, Treiber DK, Gallant P, Atteridge CE, Campbell BT, et al. A quantitative analysis of kinase inhibitor selectivity. Nat Biotechnol 2008;26(1):127–32. doi:10.1038/nbt1358.